SUPPLEMENTARY MATERIALS

CRISPR/CAS9-MEDIATED *TSPO* GENE MUTATIONS LEAD TO REDUCED MITOCHONDRIAL MEMBRANE POTENTIAL AND STEROID FORMATION IN MA-10 MOUSE TUMOR LEYDIG CELLS

Jinjiang Fan[1], Kevin Wang[1], Barry Zirkin[2] and Vassilios Papadopoulos[1,3*]

[1]Research Institute of the McGill University Health Centre and Department of Medicine, Faculty of Medicine, McGill University, Montreal, Quebec, H4A 3J1, Canada

[2]Department of Biochemistry and Molecular Biology, Johns Hopkins Bloomberg School of Public Health, Baltimore, Maryland 21205, USA

[3]Department of Pharmacology and Pharmaceutical Sciences, School of Pharmacy, University of Southern California, Los Angeles, CA 90089, USA

*Author for correspondence at vpapadop@usc.edu

Supplementary Figure Legends

Fig. S1. Validation of the CRISPR/Cas9 – mediated genome editing of mouse *Tspo* gene in MA-10 cell line(s). A - C, DNA sequencing chromatogram of each amplicon from each subcell line using *Tspo*-locus specific primers, in comparison to control wild-type (WT) cells. The covering area is as shown WT (A), nG1 (B), and G2G (C). D – G, Immunoblot analysis and RT-PCR of TSPO expression were performed using different anti-TSPO Abs and *Tspo*-specific primers, as indicated, where the G2G cells were confirmed to have no TSPO expression, where anti-HPRT (re-probing with the same membrane) was used as loading control (D); the size of *Tspo* locus-specific PCR amplicons for G2G and nG1 cells were determined using primer sets: Exon2-R/Exon2-F and Exon RR/FF (5'- TTGTAGAACTGCCCTCACCCCTACC-3' and 5'-ATTCCAGGGGCAACAGAGCACAGC-3') (E); the nG1 cells with abnormal immunoblotting band indicate that the TSPO has been mutated at genome level, in comparison to WT cells: HH and G1 (F). M, Biotinylated protein ladder; HH, the Mito-H cells (derived from MA-10 cells) with mito-roGFP; G1 and G2, the Mito-H cells transfected with gRNA1 and gRNA2, respectively; G1G and

G2G, the mito-H cells transfected with gRNA1 and gRNA2, respectively; MA-10, the MA-10 cells without any transfection; E.-I, *E. coli* cell with TSPO expression under IPTG induction. Arrow, indicate the expected missing band of TSPO in green, and unexpected band in red. The commercial RmAb, rabbit monoclonal antibody to TSPO. G. Immunoblot analysis of CYP11A1 among sub-cell lines: G1, nG1, and WT MA-10. Re-probing of the same membrane with anti-HPRT is indicated. M, Biotinylated protein ladder.

Fig. S2. Immunofluorescence staining of TSPO in the CRISPR/Cas9- mediated mutant cells nG1 and G2G, in comparison to their corresponding G1 and HH control cells. Immunofluorescence was evaluate using laser scanning confocal microscopy in control (A and C) and mutant cells (B and D). TSPO was labeled with rabbit monoclonal anti-TSPO Ab and Alexa Fluor® 546 Donkey Anti-Rabbit IgG in red for confocal images. Mitochondria were counterstained with MitoTracker™ Deep Red FM and painted in green and also shown by mito-roGFP in blue for cell HH and G2G. Scale bar: 10 μm for confocal images.

Fig. S3. Predicted putative mutant TSPO. A. Predicted peptides of the putative mutant TSPO in nG1, G2G and control cells. The 2nd likely methionine (M60) seems to be present in both mutant nG1 and G2G cells, as shown in the predicted secondary structure of TSPO in lipid membrane which shows the deletion occurred at the 1st transmembrane domain. The 2nd likely methionine: M60, indicated by red arrow, and the 2nd tyrosine involved in the formation of a covalent bond in the dual topology model is indicated in red circle. The predicted secondary structure of TSPO was produced using TMRPres2D. B. The molecular surfaces of wild-type TSPO (PDB: 2MGY) after removal of PK 11195 and minimized energy and predicted mutant TSPO (N-terminal sequence starting from the M60) with an electrostatic potential are colored by red – negative, blue – positive, and white – neutral. The mutant TSPO protein has a more neutral area in comparison with WT TSPO, which likely affects its interaction with other OMM partner, such as VDAC, and/or self aggregation or polymerization. The cholesterol recognition amino acid consensus (CRAC) sequence is indicated in green.

Fig. S4. The live mitochondria in HH and G2G cells were stained with Mitotracker Red CMXRos before and after dbcAMP treatment, where the dye accumulation depends on $\Delta\psi_m$. and fixed mitochondria in the same cells was shown under transmission electron microscopy. The “sticking”

mitochondria was observed in the G2G cells in comparison with that in HH cells (as highlighted in dotted rectangular line) (A and E). After the dbcAMP treatment, mitochondrial morphology of both cells have not dramatically changes from Mitotracker Red CMXRos staining (C and G). Overlapped images of Mitotracker Red CMXRos staining with mito-roGFP measuring mitochondrial redox status are shown (B, D, F and H).

Fig. S5. Apoptosis and cell proliferation assays of control and *Tspo*-depleted cells. A – D. A representative confocal image of live cells double stained with CellEvent Caspase-3/7 Green detection reagent (white arrow; green) and Hoechst 33342 (blue). E. Bar graph of percentages of apoptotic cells per total live cells. There is a statistically significant lower amount of apoptotic cells under TSPO deficiency (n = average 1059.3 cells/group; Bars report mean ± SEM; Student's *t* - test, $*p < 0.05$). F. A dot plot of relative proliferation of these two types of cells. No significant difference of the ratios of relative proliferation before and after dbcAMP treatment (Student's *t* - test, n = 15 wells/cell line) between these two sub-cell lines. Scale bar, 100 μm.

Fig. S6. Confocal images of STAR-DsRed fusion protein used for validation of the STAR protein mitochondrial import. STAR-DsRed protein is localized outside the mitochondria, stained with Mito-roGFP, in control HH cells (A and E) and TSPO-deficient G2G (C and G). Following 1 mM dbcAMP treatment for 2 hours, the STAR-DsRed is imported into the mitochondria in control HH cells (B and F), but a lot remains outside of the mitochondria in the TSPO mutant G2G cells (D and H). The panels A – D are highlighted from the panels E – H, respectively. Scale bar, 10 μm.

Fig. S7. A diagram of the proposed mechanism for TSPO-mediated steroidogenesis. The proposed mechanism involves the basic function of $\Delta\psi_m$ regulation via VDAC1, balanced polymerized and dimeric tubulin, and STAR mitochondrial import, both of which are involved in the transport of cholesterol into mitochondrial for steroidogenesis. In TSPO mutant nG1 cells, the STAR inhibition occurs after the dbcAMP stimulation; in the G2G cells, the STAR protein was blocked on the surface of the mitochondria; both cases were in consistent with previous proposal on the role of STAR protein on the mitochondrial surface involving in cholesterol flux into the mitochondria (1,2). $\Delta\psi_m$ that is needed for steroid biosynthesis after dbcAMP stimulation was reduced under TSPO deficiency, as shown in nG1 (middle) and G2G (right) cells.

References

1. Arakane F, Kallen CB, Watari H, Foster JA, Sepuri NB, Pain D, Stayrook SE, Lewis M, Gerton GL, Strauss JF, 3rd. The mechanism of action of steroidogenic acute regulatory protein (StAR). StAR acts on the outside of mitochondria to stimulate steroidogenesis. J Biol Chem 1998; 273:16339-16345

2. Arakane F, Sugawara T, Nishino H, Liu Z, Holt JA, Pain D, Stocco DM, Miller WL, Strauss JF, 3rd. Steroidogenic acute regulatory protein (StAR) retains activity in the absence of its mitochondrial import sequence: implications for the mechanism of StAR action. Proc Natl Acad Sci U S A 1996; 93:13731-13736

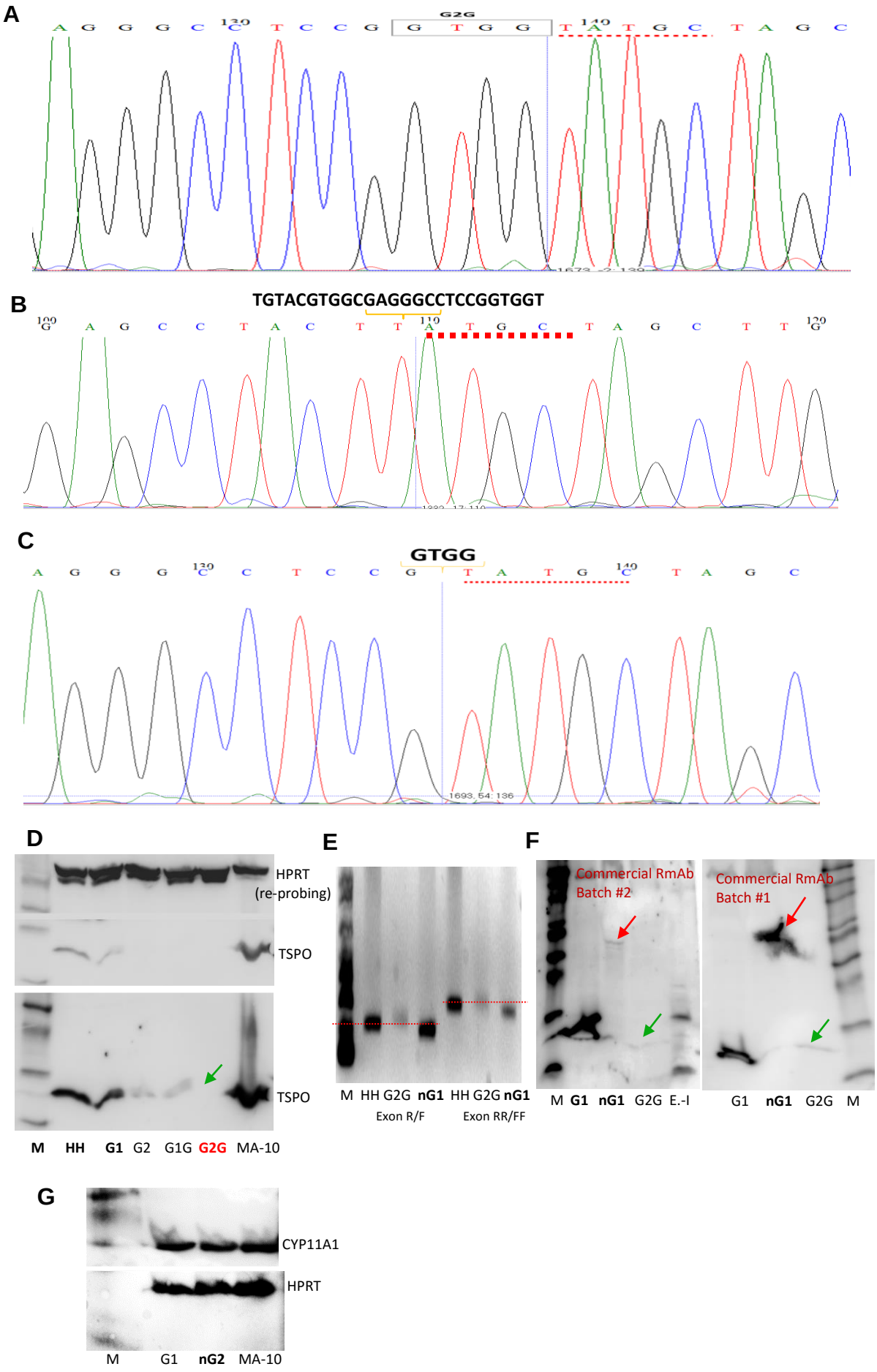
A
G2G
B
TGTACGTGGCGAGGGCCTCCGGTGGT
C
GTGG
D
HPRT
(re-probing)
TSPO
TSPO
M HH G1 G2 G1G G2G MA-10
E
M HH G2G nG1 HH G2G nG1
Exon R/F
Exon RR/FF
F
Commercial RmAb
Batch #2
Commercial RmAb
Batch #1
M G1 nG1 G2G E.-I
G1 nG1 G2G M
G
CYP11A1
HPRT
M G1 nG2 MA-10

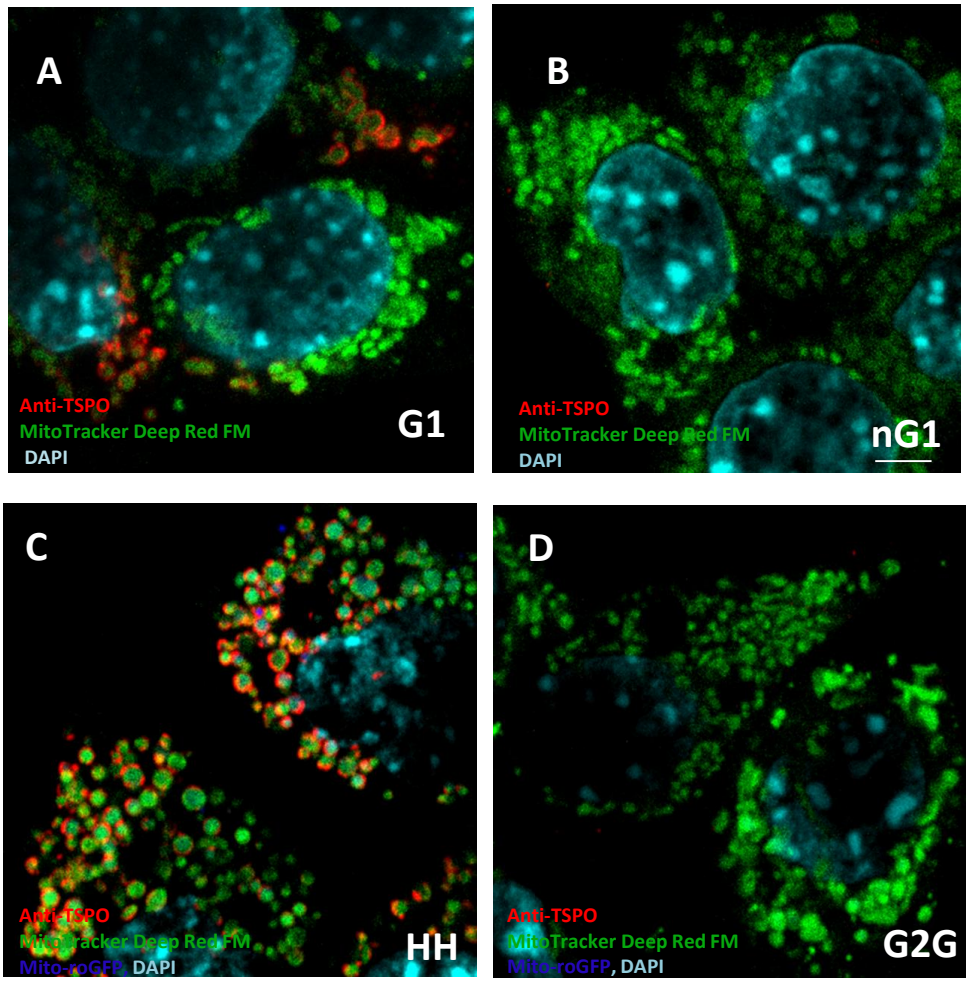
A
Anti-TSPO
MitoTracker Deep Red FM
DAPI
G1
B
Anti-TSPO
MitoTracker Deep Red FM
DAPI
nG1
C
Anti-TSPO
MitoTracker Deep Red FM
Mito-roGFP, DAPI
HH
D
Anti-TSPO
MitoTracker Deep Red FM
Mito-roGFP, DAPI
G2G

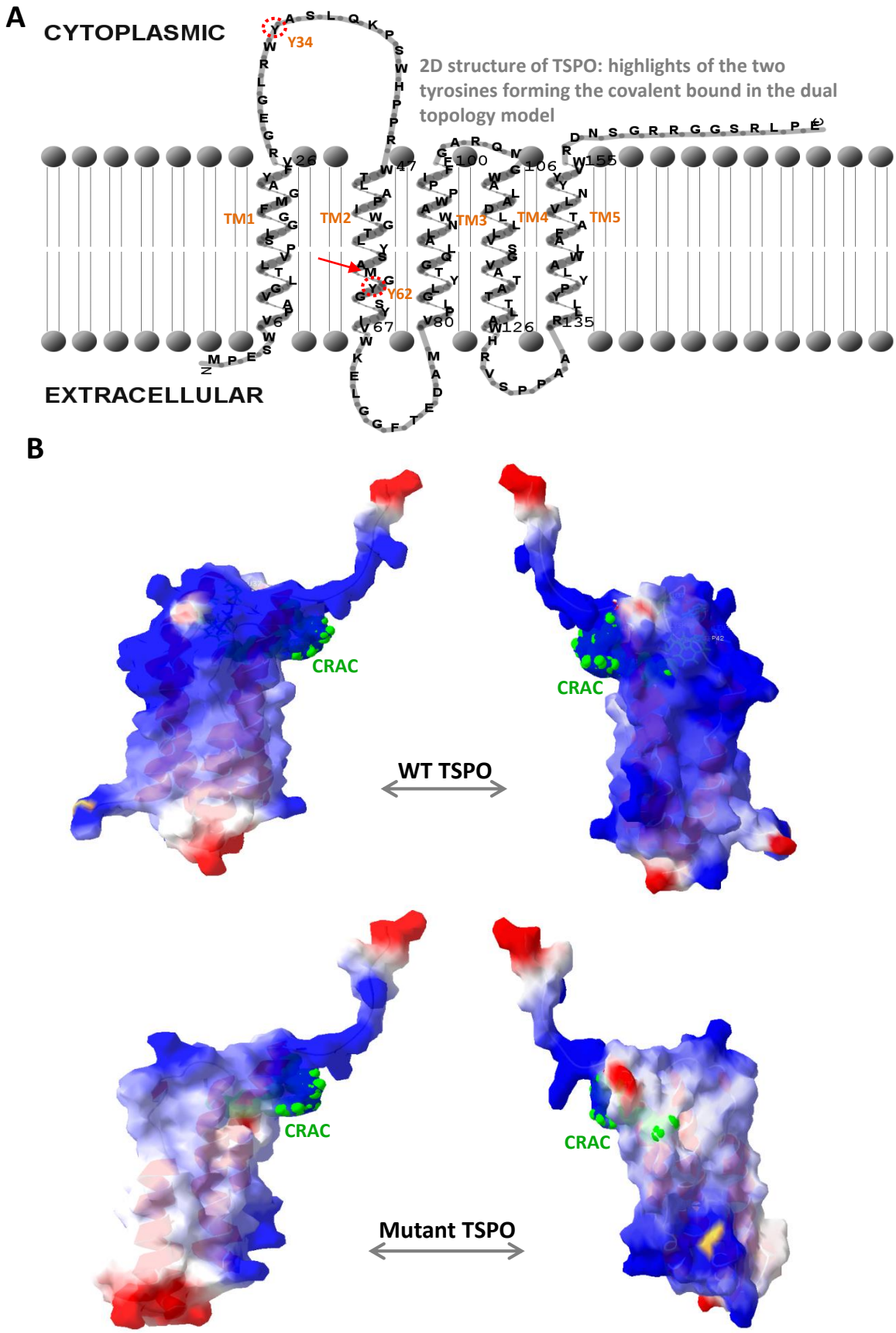
A
CYTOPLASMIC
Y34
2D structure of TSPO: highlights of the two tyrosines forming the covalent bound in the dual topology model
TM1
TM2
TM3
TM4
TM5
Y62
EXTRACELLULAR
B
CRAC
CRAC
WT TSPO
CRAC
CRAC
Mutant TSPO

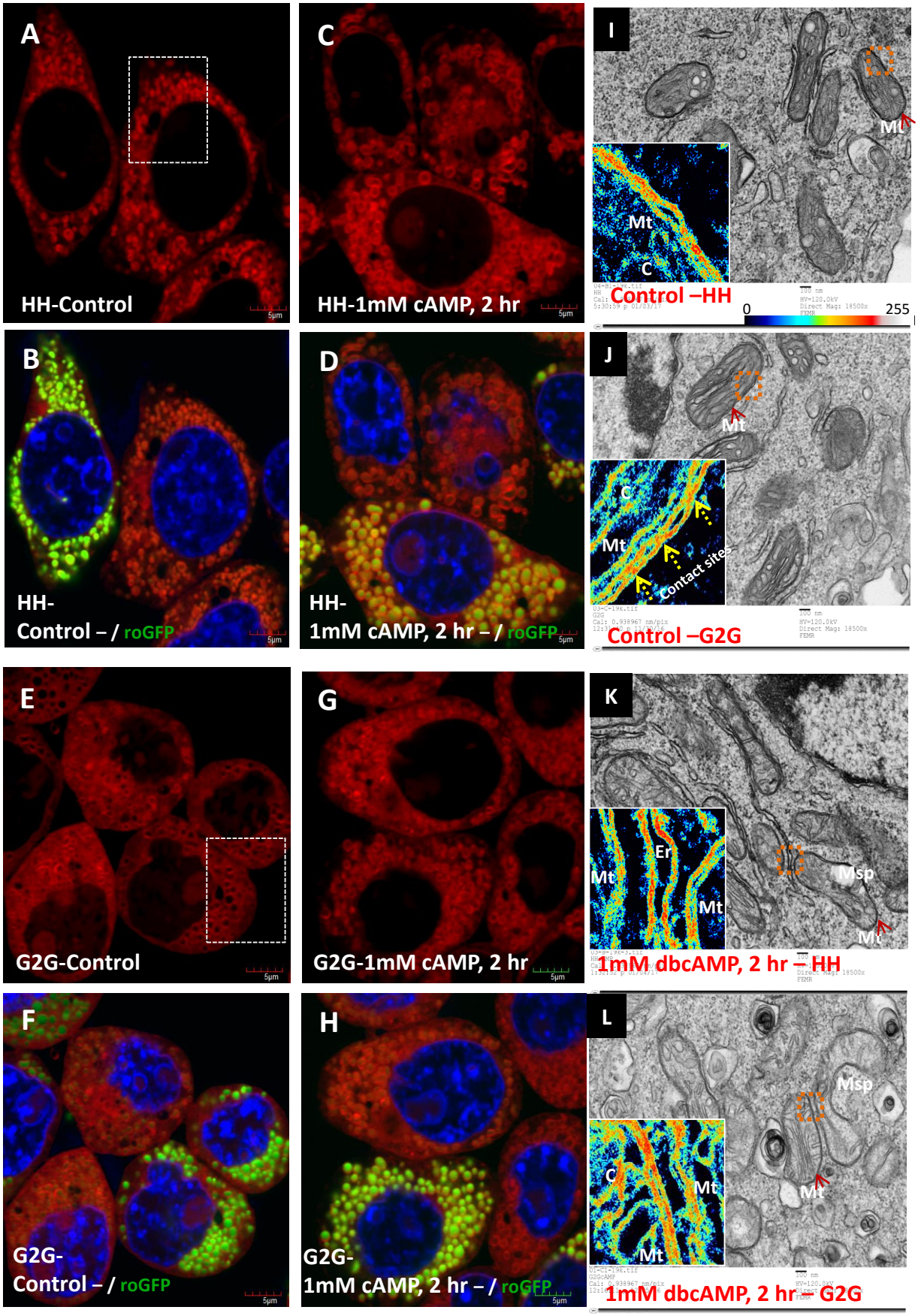
A
HH-Control
C
HH-1mM cAMP, 2 hr
I
Mt
C
Control –HH
0
255
B
HH-
Control – / roGFP
D
HH-
1mM cAMP, 2 hr – / roGFP
J
Mt
C
Mt
Contact sites
Control –G2G
E
G2G-Control
G
G2G-1mM cAMP, 2 hr
K
Er
Mt
Mt
Msp
Mt
1mM dbcAMP, 2 hr – HH
F
G2G-
Control – / roGFP
H
G2G-
1mM cAMP, 2 hr – / roGFP
L
Msp
C
Mt
Mt
Mt
1mM dbcAMP, 2 hr – G2G

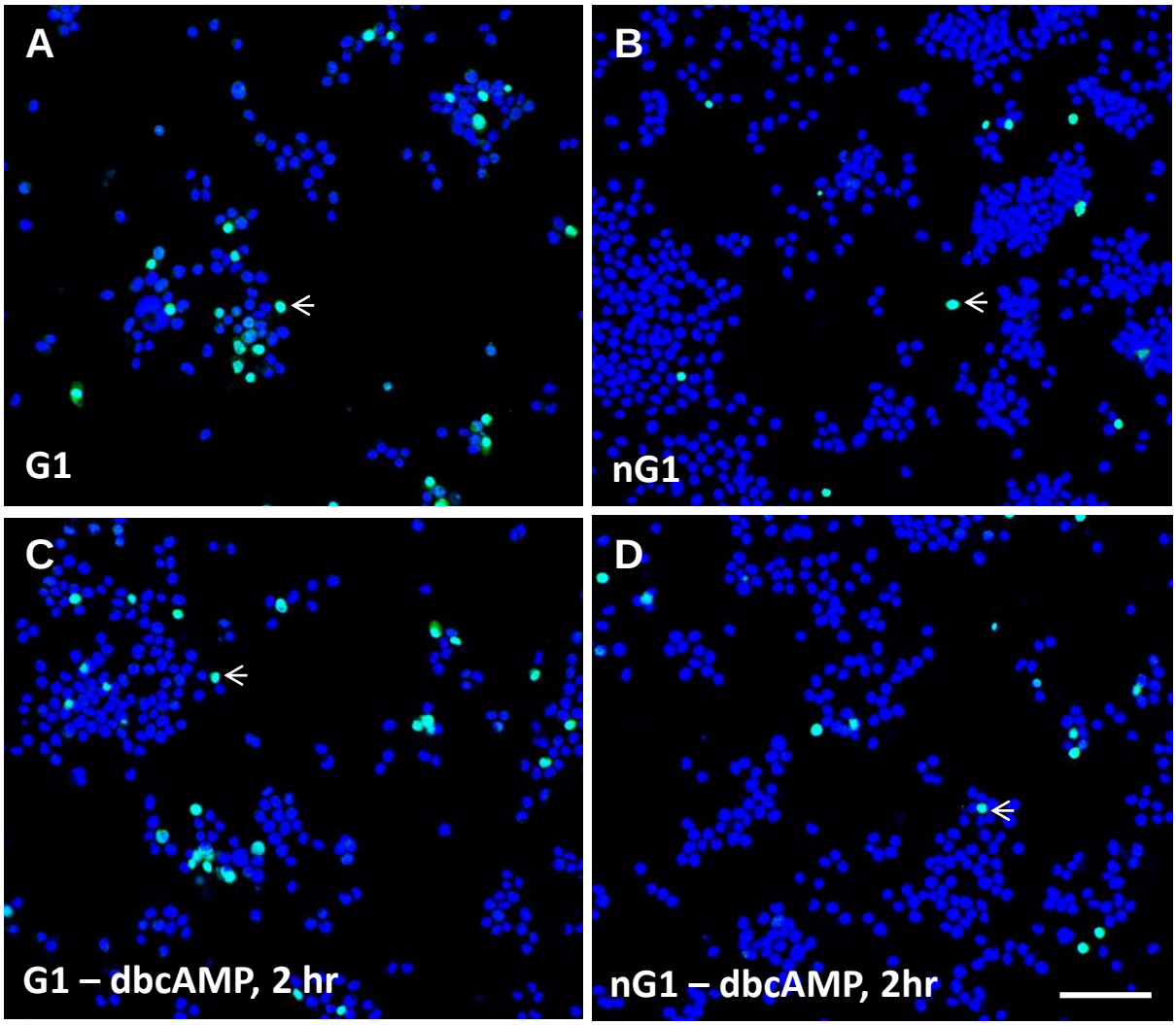
A
G1
B
nG1
C
G1 – dbcAMP, 2 hr
D
nG1 – dbcAMP, 2hr

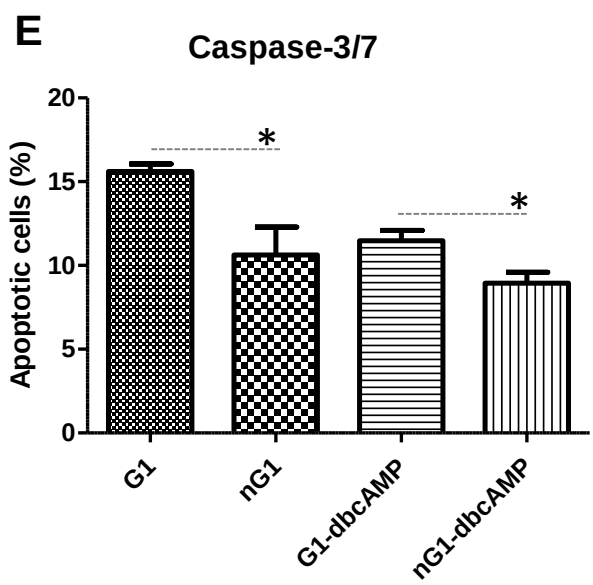
E
Caspase-3/7
Apoptotic cells (%)
20
15
10
5
0
*
*
G1
nG1
G1-dbcAMP
nG1-dbcAMP

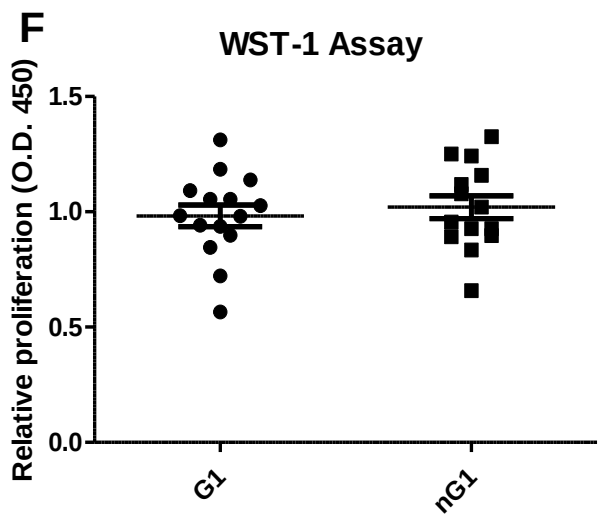
F
WST-1 Assay
Relative proliferation (O.D. 450)
1.5
1.0
0.5
0.0
G1
nG1

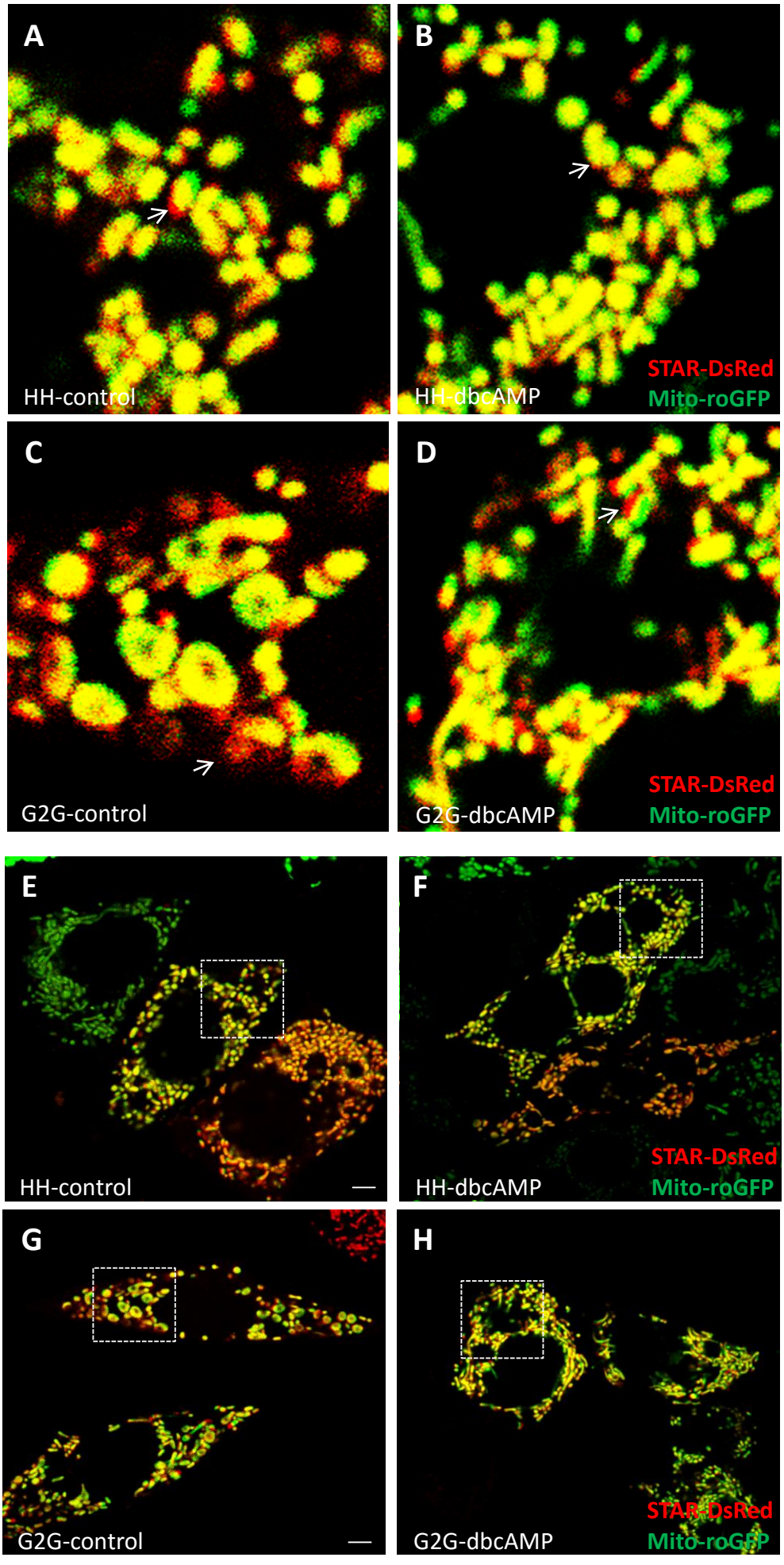
A
HH-control
B
HH-dbcAMP
STAR-DsRed
Mito-roGFP
C
G2G-control
D
G2G-dbcAMP
STAR-DsRed
Mito-roGFP
E
HH-control
F
HH-dbcAMP
STAR-DsRed
Mito-roGFP
G
G2G-control
H
G2G-dbcAMP
STAR-DsRed
Mito-roGFP

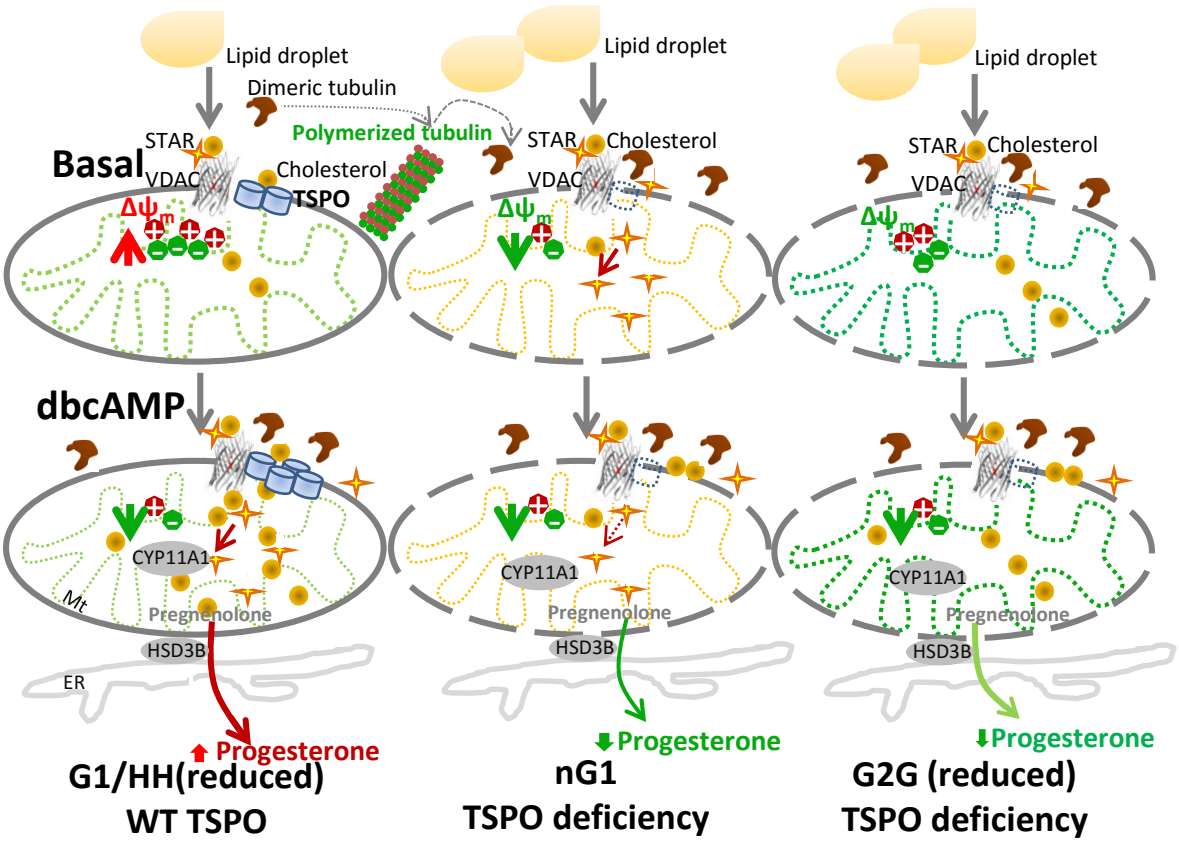
Lipid droplet
Dimeric tubulin
Polymerized tubulin
Basal
STAR
VDAC
Cholesterol
TSPO
Δψm
dbcAMP
CYP11A1
Mt
Pregnenolone
HSD3B
ER
Progesterone
G1/HH(reduced)
WT TSPO
nG1
TSPO deficiency
G2G (reduced)
TSPO deficiency